Identification of new protein-protein interactions with NUAK2 by proximity-dependent biotin labeling

Eva Domènech Moreno

Master's Thesis

Master's Degree Programme in Biotechnology
(MBIOT)

Faculty of Biological and Environmental Sciences

University of Helsinki

28th May 2017

No vuela quien tiene alas,

sino quien tiene un cielo

– Elvira Sastre

Table of contents

Abbreviations

Ala	Alanine
AMP	Adenosine 3', 5'-cyclic monophosphate
AMPK	AMP-activated kinase
AOM	Azoymethane
As160	PKB substrate 160 Da
Asn	Asparagine
ATP	Adenosine triphosphate
BioID	Proximity dependent biotin identification method
BirA	Biotin ligase A
C-terminus	Carboxyl-terminus
CCRK	Cell cycle related kinase
CD95	Cluster of differentiation 95
CDK	Cyclin-dependent kinase
CDS	Coding DNA sequence
CGH	Comparative genomic hybridization
CMV	Cytomegalovirus promoter
DMEM	Dulbecco's Modified Eagle's Medium
DMSO	Dimethyl sulfoxide
DNA	Deoxyribonucleic acid
DTT	Dithiothreitol
EDTA	Ethylenediaminetetraacetic acid
FA	Fatty acid
FBS	Fetal bovine serum
GFP	Green fluorescent protein
GLUT4	Glucose transporter type 4
Gly	Glycine
GTP	Guanosine-5'-triphosphate
HEK	Human embryonic kidney cells
ICK	Intestinal cell kinase
ICK TA	Intestinal cell kinase mutated
kDa	Kilo daltons
KO	Knock out
LKB1	Liver kinase B1
MARK1-4	Microtubule-affinity regulated kinase 1-4
MEF	Mouse embryonic fibroblast
MELK	Maternal embryonic leucine zipper kinase
MLC	Myosin light chain
MO25	Calcium-binding protein 39
MRIP	Myosin Rho interacting protein
mTOR	Mammalian target of rapamycin complex
MYPT1	Myosin phosphatase targeting I
N-terminus	Amino-terminus
NFκB	Nuclear factor kappa-light-chain enhancer of activated B cells
NUAK1-2	Novel sucrose non-fermenting kinase 1-2
PAGE	Polyacrylamide gel electrophoresis
PBS	Phosphate buffered saline
PCR	Polymerase chain reaction
PJS	Peuth-Jeghers Syndrome
PKB	Protein kinase B
PP1	Protein phosphatase I
PTEN	Phosphatase and tensin homolog
RhoA	Ras homolog gene family, member A
ROCK	Rho-associated protein kinase
rpm	Revolutions per minute
SAP	Shrimp Alkaline Phosphatase
SDN	SNARK dominant negative mutant kinase
SDS	Sodium dodecyl sulfate
Ser	Serine
SIK1-3	Salt inducible kinase 1-3
SNARK	Sucrose-non-fermenting AMPK-related kinase
SNF1	Sucrose non-fermenting 1
SNRK	SNF1-related kinase
STK11	Serine-threonine kinase 11
STRAD	Ste20 related adaptor
TBC1D1	TBC domain family member 1
TBC1D4	TBC domain family member 4
TBS	Tris buffered saline
TetO	Tetracycline operator
Thr	Threonine
TNFα	Tumor necrosis factor alpha
tTA	Tetracycline transactivator

Abstract

In this Master's project, I have studied a mammalian serine-threonine kinase NUAK2 implicated in human disease but whose molecular functions and interacting proteins are as of yet poorly characterized. The goal was to identify new interacting proteins to increase understanding of the molecular functions and potentially link to human physiology and disease. Recent work from the host lab shows NUAK2 loss in cultured primary cells mimics loss of the tumor suppressor LKB1 which also acts upstream of NUAK2, together suggesting NUAK2 could be involved in tumor suppression.

Currently, only two protein-protein interacting proteins with NUAK2 have been identified: NUAK2 is targeted to actin stress fibers by the myosin phosphatase Rho-interacting protein (MRIP), and it is involved in regulating cell contractility by affecting indirectly the phosphorylation cycle of the myosin light chain through inactivation of the myosin phosphatase target subunit 1 (MYPT1).

In this project, I utilized a novel protein-protein interaction screening method that utilizes proximity-dependent biotin labeling to identify new interacting proteins with NUAK2 in human embryonic kidney cells (HEK 293). This method is based on fusing an *E.Coli* promiscuous biotin ligase, $BirA^{*(R118G)}$, to the investigated protein. The $BirA^{*(R118G)}$ ligase biotinylates all the proteins in close proximity of the fusion protein creating a history of protein-protein associations over time. Afterwards, the biotinylated proteins can be isolated by affinity purification methods and identified by mass-spectrometry.

The screening identified the previously known interaction partners of NUAK2 indicating it was technically successful. In addition, I also identified in total 108 novel potential protein interaction partners for NUAK2. One of the top hits was Cytospin-A, a cross-linking protein between microtubules and actin cytoskeleton, supporting a role of NUAK2 as regulator of cytoskeleton. Supporting the validity of our finding, Cytospin-A depletion in mammalian cells causes defective actin-cytoskeleton reorganization, a very similar phenotype seen with NUAK2 depletion.

In future studies, I will continue to investigate the specific role of NUAK2 and Cytospin-A aiming for detailed information on the function of NUAK2 in regulation of microtubules and actin cytoskeleton. Validation of some of the other identified interactions is expected to provide novel insights to the biology and role of NUAK2 in LKB1 tumor suppressor functions.

Key words: NUAK2, LKB1, protein-protein interactions, proximity-dependent biotin labeling, BioID, tumorigenesis.

1 Background

1.1 Kinases are key players in cell signaling in human physiology and cancer cells

All essential cellular processes like cell growth, proliferation, or differentiation are determined by dynamic integration and response to extracellular and intracellular signals. Cells are constrained to their environment and their behavior is tightly influenced by it. Phosphorylation is one of the fundamental signaling transduction mechanisms cells use to integrate and propagate information. Addition of phosphate groups to molecules is a post-translational modification and it usually modifies the conformational structure of the target molecule and therefore it alters its function e.g. by changing affinity or reactivity to other molecules. Phosphorylation is controlled by transient interactions between protein kinases and their substrates. Protein kinases comprise a big family of signaling proteins and they are found in all living organisms (Grangeasse et al., 2012; Wang et al., 2010). The human genome contains 500 genes that encode tyrosine or serine-threonine protein kinases, comprising up to 2% of all genes (Manning et al. 2002). The phosphorylation signals are often propagated and amplified through cascades of several kinases that are phosphorylated sequentially. Detection and identification of all these transient interactions is challenging as they are highly dynamic and fast.

Since phosphorylation events are involved in all essential cellular processes it is not surprising that tumor cells often have many of the protein kinases or their counterparts, protein phosphatases, mutated. Tumor cells need to hijack their signaling network to constitutively activate growth and proliferation programs as well as to inactivate suicidal behavior, apoptotic programs that otherwise are triggered when the cell detects that its signaling has been compromised (Fleuren et al., 2016).

NUAK2 is a substrate of the tumor suppressor kinase LKB1. The molecular mechanisms by which LKB1 functions as a tumor suppressor remain unknown, in part due to limited knowledge of the protein-protein interactions of its substrates. Loss of NUAK2 in cultured primary cells resembles loss of LKB1 suggesting NUAK2 could be involved in tumor suppression. Therefore, identifying new partners for NUAK2 can bring light to understand its biological functions and its involvement in tumorigenesis.

1.2 Regulation of NUAK2

1.2.1 NUAK2 is a substrate of the tumor suppressor kinase LKB1

NUAK2, also known as sucrose-non-fermenting AMPK-related kinase (SNARK), is a serine-threonine kinase of 76 kDa. It was first identified as an ultraviolet induced gene in rat keratinocytes in 2001 (Lefebvre et al., 2001). NUAK2 belongs to a group of 12 other kinases closely related to the energy

sensor AMP-activated kinases (AMPK) subunits α1 and α2. These kinases have been commonly grouped as AMPK subfamily or AMPK-related kinases. Their main feature is a conserved kinase catalytic domain (**Figure 1**) (Lizcano et al., 2004). Within the AMPK subfamily, NUAK2 is more closely related to the kinase NUAK1. These two kinases differ from the rest of the AMPK subfamily in that they lack an ubiquitin associated domain after the C-terminus of the kinase domain (Katajisto et al., 2007). Even though mammals have two different genes, *C.Elegans* has a unique orthologue, UNC-82 (Hoppe et al., 2010), suggesting NUAK1 and NUAK2 likely derived from a common ancestor gene and therefore they could still share cellular functions and interaction partners.

The AMPK-related kinases, with the exception of MELK, are strongly activated *in vitro* by phosphorylation of a conserved T-loop threonine residue by an upstream serine-threonine kinase, LKB1 (**Figure 1**). Full activation of LKB1 kinase activity and subsequent substrate activation requires the formation of a complex with the scaffold MO25 protein and the pseudokinase STRAD as this complex stabilizes and localizes LKB1 in the cytoplasm (Lizcano et al., 2004). Endogenous activity of the AMPK-related kinases was dramatically decreased in cells that did not express LKB1 or where LKB1 was previously depleted, suggesting LKB1 is a limiting factor in AMPK-related kinases activation, at least *in vitro* (Lizcano et al., 2004).

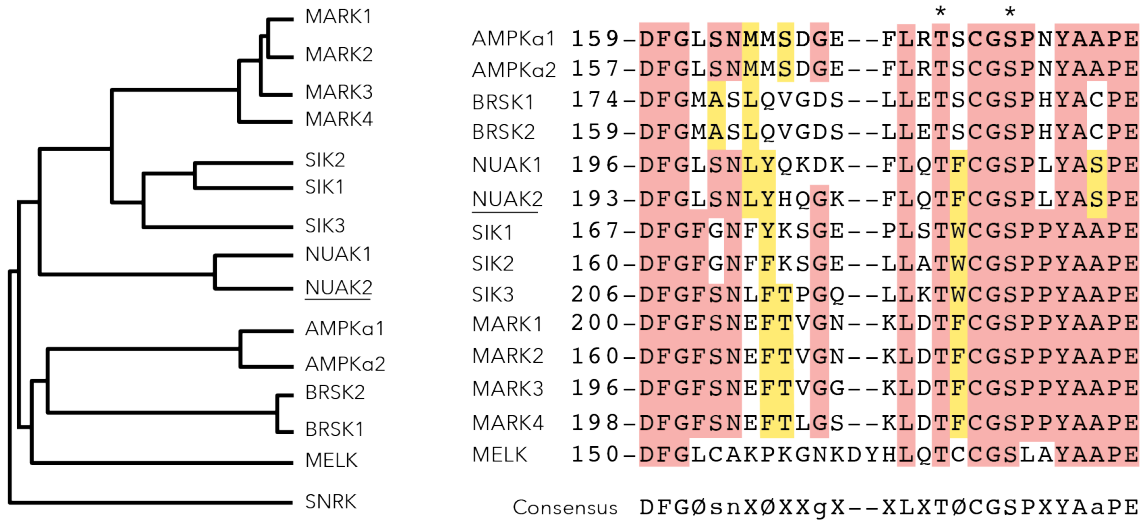

Figure 1: Dendogram and alignment of the T-loop sequences of the AMPK-related kinases. *Identical residues are marked in red and conserved residues are marked in yellow. Asterisk indicates the Thr and Ser phosphorylation sites of LKB1. The consensus sequence is the optimal sequence for LKB1 phosphorylation suggested by Lizcano et al., 2004. X stands for any aminoacid; ∅ represents a large hydrophobic residue; a, g, n, and s indicate*

preference for Ala, Gly, Asn and Ser, respectively. (Dendogram modified from Cell Signaling Technologies (www.cellsignal.com) and T-loop sequences adapted from Lizcano et al., 2004)

1.2.2 NUAK2 expression is induced by several cell stresses

AMPK is part of the stress response system of the cells. As its homolog in yeast SNF1, AMPK expression is induced by different cell stresses like hypoxia, glucose deprivation or increased intracellular AMP:ATP ratio (Hardie, 2007). Induction of AMPK by cellular stresses and further activation by LKB1 phosphorylation triggers a signaling cascade that through inactivation of the mammalian target of rapamycin (mTOR) switches off cellular anabolic pathways and prepares the cell to restore energy storage through catabolic metabolism (Xu et al., 2012). Of other kinases of the AMPK subfamily, only NUAK2 has been found to respond to several cellular stresses. NUAK2 expression in several cell lines is induced by nutrient deprivation, like glucose or glutamine deficiency, hypoxia conditions or increased reactive oxygen molecules (Lefebvre and Rosen, 2005). However, unlike AMPK, this response to cellular stress seems to be highly cell context and cell type dependent as several studies have highlighted (Lefebvre et al. 2001; Lizcano et al. 2004; Lefebvre and Rosen 2005). In human myocyte cultures, NUAK2 expression is induced by TNFα and palmitate, two stress molecules involved in the acquirement of insulin-resistance by skeletal muscle cells (Rune et al., 2009). Even though this insulin-resistance was found to be independent of NUAK2 status, as discussed in next section, there is more evidence to suggest NUAK2 has a role in skeletal muscle metabolism homeostasis, and that it mediates part of the exercise-stimulated glucose transport (Koh et al., 2010).

1.3 Functions of NUAK2

1.3.1 Role of NUAK2 in skeletal muscle cell metabolism

Skeletal muscle cells are key players in glucose homeostasis as they are major consumers and storage of glucose in adults. Insulin and exercise are the two main stimulators of glucose transport in muscle cells. It is well known that in situations of insulin-resistance like diabetes type 2, where insulin-stimulated glucose transport is impaired, exercise is highly beneficial as it increases glucose uptake and transport in skeletal muscle cells, as well as insulin sensitivity and fatty acid (FA) oxidation (Stanford and Goodyear, 2014). Insulin and exercise stimulation of glucose transport act through different signaling pathways but their signaling converge at the protein kinase B (PKB) substrates paralogs, AS160 (also known as TBC1D4) and TBC1D1 increasing their phosphorylation and promoting an increase of the glucose transporter (GLUT4) translocation from vesicles to the plasma membrane (Goodyear and Kahn, 1998).

Studies using LKB1 muscle-specific knockout mice have identified LKB1 as an important molecular regulator of contraction-stimulated glucose transport. Depletion of LKB1 in skeletal muscle in mice decreased FA oxidation during treadmill exercise and decreased contraction-stimulated glucose transport (Koh et al., 2006). These mice also had reduced AMPKα2 (the predominant AMPK subunit in muscle) and lower phosphorylation of AS160 and TBC1D1 (Jeppesen et al., 2013). Even though AMPKα2 was dramatically reduced, and was thought to be the sole substrate of LKB1 involved in glucose metabolism, further studies using mice lacking AMPKα2 have revealed that AMPK cannot be the only LKB1 substrate involved in contraction-stimulated glucose transport. Mice lacking AMPKα2 only had partially decreased FA oxidation and a slight, or no change at all, in exercise-dependent glucose uptake and transport stimulation (Fujii et al., 2005; Jørgensen et al., 2004; Mu et al., 2001). These results suggested that LKB1 regulation of glucose homeostasis in muscle cells likely involved more than one member of the AMPK subfamily besides AMPKα2.

Interestingly, NUAK2 heterozygous knockout mice showed premature onset of obesity along with increased fat mass, hyperglycemia and hyperinsulinemia (Koh et al., 2010; Tsuchihara et al., 2008), all classic features of glucose intolerance and diabetes type 2. Moreover, these mice showed reduced contraction-stimulated glucose transport when tested for treadmill exercise, and myocytes derived from these mice had also lower phosphorylation of TBC1D1 (Koh et al., 2010). In the same line, mice expressing a dominant negative mutant NUAK2 also had impaired contraction-stimulated glucose transport suggesting NUAK2 is a specific LKB1 substrate regulating contraction-stimulated glucose transport in skeletal muscle cells (Koh et al., 2010). In addition to these studies, obese people have also increased levels of NUAK2 in muscle cells and as mentioned before, NUAK2 was severely increased when human myocyte cell cultures were exposed to TNFα and palmitate, agents that induce insulin resistance (Rune et al., 2009). Acquirement of insulin resistance was independent of NUAK2 levels, as depletion of NUAK2 did not revert insulin resistance suggesting induction of NUAK2 in human obesity is more likely to be a response to counterbalance insulin resistance effects by increasing exercise-dependent glucose uptake and transport (Rune et al., 2009).

1.3.2 NUAK2 promotes actin stress fibers remodeling

Currently, there are only two known proteins that physically interact with NUAK2. Both of these proteins belong to the regulation of the phosphorylation cycle of the myosin light chain (MLC) at the actin stress fibers of smooth muscle cells. Changes in ATPase activity of MLC remodels the actin stress fibers changing contractility and motility of cells (Kreisberg et al., 1997). Increased phosphorylation of MLC causes higher contraction of the actin bundles and subsequent cell detachment and increased cell motility.

This phosphorylation is classically regulated by Rho kinase proteins (ROCK), serine/threonine kinases that are activated by an upstream small GTPase, RhoA (Kreisberg et al., 1997). Desphosphorylation of MLC is carried out by MLC phosphatase. This protein complex is comprised of a phosphatase regulatory subunit (MYPT1) and a phosphatase catalytic subunit (PP1). The MLC phosphatase as well as RhoA are recruited to actin stress fibers by the myosin Rho interacting protein (MRIP) (Surks et al., 2005).

MRIP also recruits NUAK2 to the same location (Vallenius et al., 2011). This interaction is needed for NUAK2 inhibition of the phosphatase regulatory subunit (MYPT1) function. The fact that presence of NUAK2 at the actin stress fibers prevents dephosphorylation of MLC is thought to be partially kinase-independent, as an inactive kinase mutant NUAK2 succeeded to inhibit the phosphatase action (Vallenius et al., 2011). However, an independent study has also showed that NUAK2 can directly bind and phosphorylate MYPT1 (Yamamoto et al., 2008), indicating that NUAK2 might inhibit the phosphatase also in a kinase-dependent manner. In a similar model, the related kinase, NUAK1, has also been reported to physically interact with the MLC phosphatase complex, in this case with the catalytic subunit PP1, and inactivate the phosphatase by direct phosphorylation of the Ser^{445}, Ser^{472} and Ser^{910} residues of MYPT1, all different sites than the usually phosphorylated by ROCK (Thr^{696}, Thr^{853}) (Zagórska et al., 2010). Phosphorylation of MYPT1 recruits the phosphatase to scaffold 14-3-3 proteins that trap and keep the phosphatase away from the actin stress fibers and therefore prevents dephosphorylation of MLC (Koga and Ikebe, 2008; Zagórska et al., 2010). These slightly different models suggest NUAK kinases might collaborate or have redundant functions at the actin stress fibers. In both scenarios, the presence of NUAKs at the actin stress fibers increases turnover, cell detachment and cell motility by keeping phosphorylated the MLC (**Figure 2**). In the same line, another study has showed that overexpression of NUAK2 in a human cancer cell line causes acute cell-cell detachment when the cells are exposed to glucose-free medium (Suzuki et al. 2003).

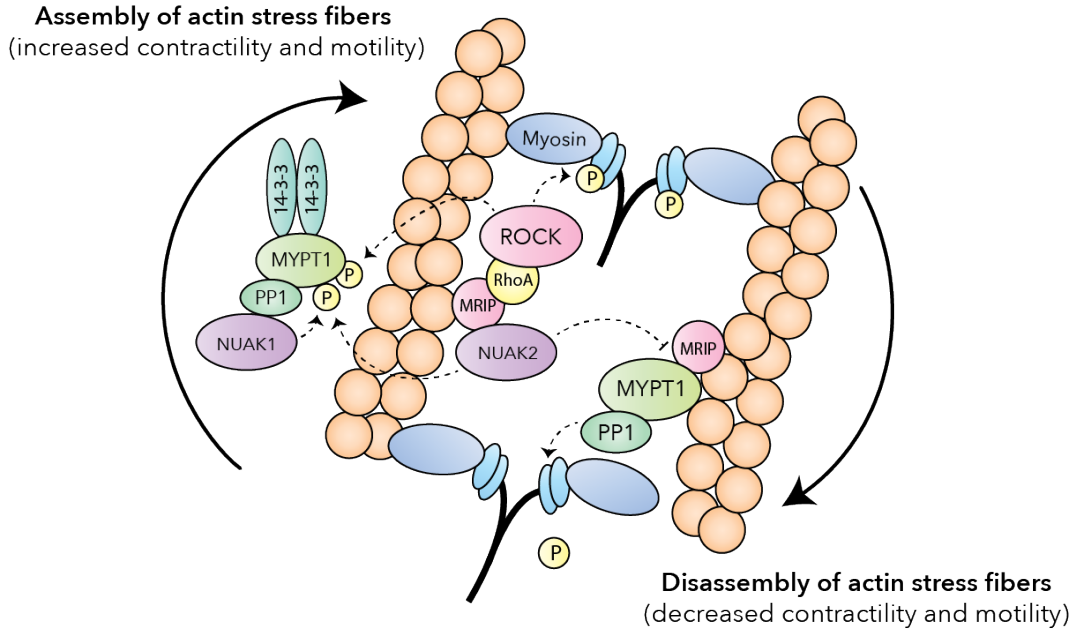

Figure 2: Proposed model of NUAK kinases role in actin stress fibers formation. *NUAK kinases increase assembly of actin stress fibers by inhibiting the MLC phosphatase complex comprised of MYPT1 and PP1 subunits. NUAK2 has been shown to inhibit the phosphatase by direct phosphorylation of MYPT1 but also in a kinase independent manner, likely to be allosteric inhibition for MRIP binding (indicated by blunted arrow). In the other hand, NUAK1 has been shown to directly interact with PP1 subunit and phosphorylate MYPT1. Phosphorylation of MYPT1 by NUAK kinases or by ROCK kinases recruits 14-3-3 proteins that keep the MLC phosphatase away from actin stress fibers, promoting stress fibers formation. Currently, MYPT1 and MRIP are the only two known protein-protein interactions with NUAK2. Actin filaments shown in orange and myosin heads in blue (MLC in cyan). Dashed arrows indicate phosphorylation event (Koga and Ikebe, 2008; Vallenius et al., 2011; Y. Wang et al., 2009; Yamamoto et al., 2008; Zagórska et al., 2010).*

1.3.3 Role of NUAK2 in apoptosis and cell survival

In addition to its role in regulating exercise-stimulated glucose transport, NUAK2 has also been shown to play a role in maintaining skeletal muscle mass (Lessard et al., 2017). Adult mice and humans displayed increased expression of NUAK2 in skeletal muscle upon aging and also in response to metabolic stress. Interestingly, the loss of NUAK2 also increased sensitivity of myocyte cultures to induced-palmitate apoptosis (Lessard et al., 2017). Moreover, mice carrying a muscle-specific NUAK2 dominant negative mutant kinase (SDN) had severe atrophy of muscle fibers (Lessard et al., 2017). Mechanistically, Lessard *et al.* showed these mice have impaired Rho signalling as they had decreased phosphorylation of MYPT1

Rho kinase Thr^{696} phosphorylation site and decreased expression of downstream Rho signalling targets, suggesting that defective Rho signalling may be involved in the apoptotic phenotypes upon NUAK2 loss. *In vitro*, primary myocytes cultures derived from SDN mice also showed the same pattern. When myocytes were exposed to palmitate, increased MYPT1 phosphorylation was observed and this effect was lost when NUAK2 was depleted from the cells (Lessard et al., 2017). It is well known that Rho/ROCK signalling is involved in apoptosis as it is required for formation of the apoptotic bodies and cell detachment (Street and Bryan, 2011). Constitutive ROCK activation is carried out by caspases that cut the regulatory domain at the C-terminus of the kinase. ROCK over-activation increases cell contraction and bud formation, characteristic of apoptotic cells, as well as cell detachment (Street and Bryan, 2011). ROCK inhibitors have been exploit as tumor therapy drugs because tumor cells use ROCK over-activation to rearrange their cytoskeleton and acquire cell invasion and metastatic properties (Street and Bryan, 2011). Here, NUAK2 could be a linking protein between apoptosis cascade and actin stress fibers remodelling.

The protective role of NUAK2 in cell survival has also been studied in tumour cells resistant to CD95 induced apoptosis (Legembre et al., 2004). Tumor cells resistant to CD95 apoptosis also show increased motility and invasiveness through activation of NFκB genes. NUAK2 was identified as one of the CD95 induced up-regulated genes. Overexpression of NUAK2 protected cells from CD95 induced apoptosis in a NFκB dependent manner, and tumor cells lacking NUAK2 were more susceptible to CD95 apoptosis. Moreover, this cells also showed a decreased motility and invasiveness capacity (Legembre et al., 2004). In a similar line, the closely related NUAK1 has also been associated to apoptosis regulation as it is activated by PKB to promote cell survival in glucose starvation situations *in vitro* (Suzuki et al. 2003).

1.4 Suggested functions of NUAK2 in tumorigenesis

As mentioned, NUAK2 is activated by the tumor suppressor kinase LKB1 along with 11 other AMPK-related kinases. Inactivation mutations of LKB1 are frequently found in sporadic lung adenocarcinomas where inactivation increases tumor proliferation and metastases (Ji et al., 2007). Moreover, LKB1 inactivation mutations underlie a hereditary condition, Peuth-Jeghers Syndrome (PJS), characterized by an increased predisposition to cancer and development of gastrointestinal polyposis (Giardiello et al., 2000). Studies in the host lab have shown that depletion of LKB1 restricted only to stromal cells is sufficient to fully develop gastrointestinal polyposis in mice, resembling PJS polyposis (Katajisto et al., 2008). Loss of LKB1 in mouse embryonic myofibroblasts causes contractility defects, shown by loss of actin stress fibers and aSMA (Vaahtomeri et al., 2008). However, the molecular mechanisms by which

LKB1 functions as a tumor suppressor remain unknown. Interestingly, NUAK2 along with NUAK1 are the LKB1 substrates involved in actin cytoskeleton dynamics, and depletion of NUAK2 also causes a reduction of actin stress fibers in MEFs (unpublished). Moreover, NUAK2 activity *in vitro* was dramatically reduced in absence of LKB1 and the NUAK2 derived T-loop peptide was a better substrate for LKB1 phosphorylation than AMPKα1 derived T-loop peptide (Lizcano et al., 2004). Together brings NUAK2 as one of the best candidates to mediate LKB1 function in stromal cells. In this line, a study using heterozygous NUAK2 mice revealed that these mice were more susceptible to azoymethane-induced (AOM) colonic tumorigenesis (Tsuchihara et al., 2008).

Contrarily to the putative tumor suppressor function of NUAK2 in gastrointestestinal tract, the literature of NUAK2 role in tumorigenesis is quite contradictory. Of the known biological functions of NUAK2, its involvement in cell survival and cell detachment as well as induction by metabolic stressors strongly suggests NUAK2 could play a prominent role as pro-tumorigenic kinase in tumor cells. Indeed, NUAK2 locus resides in chromosome 1q32, a region frequently amplified in human melanomas (Namiki, Coelho, et al., 2011). Accordingly, high levels of NUAK2 have an impact on survival rate of patients with acral melanomas and correlates with bad prognosis (Namiki, Coelho, et al., 2011). Moreover, using array-CGH it has been identified that NUAK2 is amplified along with PTEN deficiency in a subset of melanomas and that this combination promotes melanoma cell proliferation through cyclin-dependent kinases (CDK) activation (Namiki et al., 2015). In addition, inhibition of NUAK2 in mice suppressed melanoma tumour growth (Namiki, Tanemura, et al., 2011).

It is likely that NUAK2 dual role in tumorigenesis, as what happens with its regulation by cell stress, is highly cell context and cell type dependent, increasing the complexity of this kinase and putative future development of drug therapies.

1.5 Proximity-dependent biotin labeling is a novel method to study protein-protein associations in vivo

One of the challenges of this century is to characterize and map the whole network of intracellular protein-protein interactions, known as the cellular interactome. Knowing the structure and functional domains of a protein is often not enough to decipher its function inside the cell. To understand its biological relevance is more useful to identify its associations and partners and how they change over time. However, very often these interactions are weak, fast, transient, and highly cell context dependent making it challenging to successfully detect them. Proximity-dependent labelling by modifying enzymes is an approach that has been developed recently to screen and successfully identify these transient protein-protein interactions. Different modifying enzymes have been utilized, but all are based on the

same idea, to attach to a bait protein a small enzyme capable of tagging vicinity proteins by covalently modifying them (Rees et al., 2015). Afterwards the tag is used to isolate the covalently modified proteins by traditional affinity purification methods and further identify them by mass-spectrometry analysis. The BioID assay is one type of proximity-dependent labeling method based on biotin labeling, and it is the one I have used in this project to screen for new interactors with NUAK2.

The BioID method was developed in 2012 by Roux *et al.* and it is based on a small modified bacterial biotin ligase, $BirA^{*(R118G)}$. This biotin ligase mediates the biotinylation process in a two-step reaction manner. During the first step, the biotin gets activated in the enzyme pocket site, by binding to ATP (biotinoyl-5'-AMP). In the second step, this unstable biotin reacts to a protein lysine residue creating an amide bond between the biotin and the lysine chain. The modified $BirA^{*(R118G)}$ has lower affinity to the reactive biotin and it releases the molecule from its catalytic pocket prematurely. The reactive biotinyol-5'-AMP is unstable and rapidly interacts with any vicinity protein that has exposed a lysine residue. During the time the protein construct is expressed, the BirA keeps track of proteins that have passed nearby the protein of interest tagging them with biotin. Biotinylated proteins can easily be isolated by streptavidin affinity purification and identified by mass-spectrometry analysis (**Figure 3**) (Roux et al., 2012).

One of the advantages of this method is that the protein of interest is expressed in the same organism so all the post-translational modifications can occur as long as the BirA does not interfere allosterically. Moreover, biotinylation is a very stable covalent modification and cells can be lysed with stringent methods, opening the possibility to study insoluble or inaccessible cellular structures like centromeres and nuclear lamina (Firat-Karalar et al., 2014; Fu et al., 2015). The method is not exempt from a few limitations. It is still an overexpression assay, and as often happens with overexpression analysis, the protein product might be toxic for the cells or aggregate in the wrong location. The fusion construct can also affect post-translation modifications and the size of BirA, taking as reference the 27 kDa of GFP, is a bit bigger (35 kDa) so it can also affect folding and normal function of the protein. Recently, the same lab has released a smaller version of the biotin ligase to try to improve and reduce these limitations (Kim et al., 2016). All the potential problems mentioned need to be taken into account and functional validation of the fusion proteins by immunofluorescence and western blot is required prior to carrying out the whole BioID assay. Nonetheless, since the method was published in 2012, the BioID has extensively been used for a high variety of proteins and it has successfully served to study cellular structures that previously were quite troublesome, like centromeres, the nuclear complex pores or the nuclear lamina (Firat-Karalar et al. 2014; Kim et al. 2014; Fu et al. 2015).

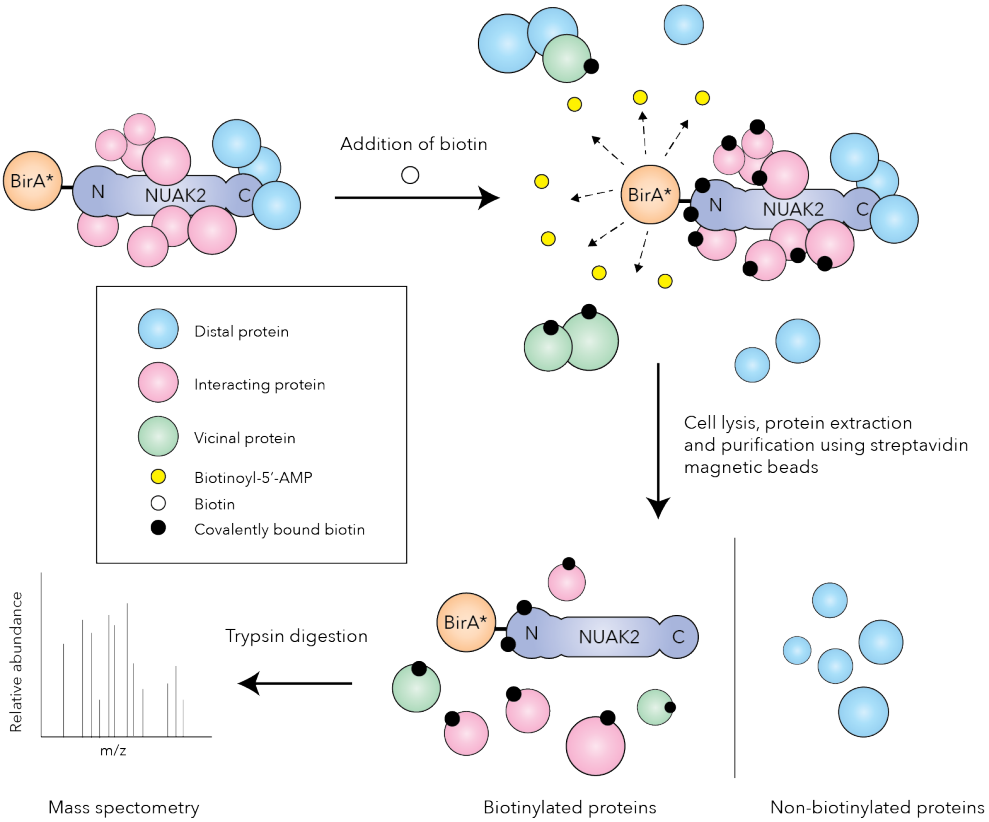

Figure 3: BioID assay. *This proximity-dependent labeling method is based on the fusion of a promiscuous biotin ligase BirA*$^{*(R118G)}$ *to the protein of interest, represented here with NUAK2. This mutant BirA*$^{*(R118G)}$ *is able to biotinylate nonspecifically vicinity proteins overtime. The fusion protein construct is transfected in the cells and after 24 h incubation with media supplemented with biotin the cells are lysed and the biotinylated proteins can be isolated using streptavidin affinity purification methods. Finally, the biotinylated proteins can be identified by mass-spectrometry (Modified from Varnaitė and MacNeill, 2016).*

2 Aims of the study

This Master's thesis focuses on identification of novel protein-protein interactions of the NUAK2 kinase with an aim to:

I. Provide insight on NUAK2 biological function through identification of proteins NUAK2 interacts with in mammalian cells.
II. Provide insight on whether NUAK2 is involved in tumor suppression.

3 Material and methods

3.1 Cell lines

I used human embryonic kidney cells (HEK 293) for transient transfections and a Flp-In T-Rex 293 cell line for generation of stable cell lines expressing the different fusion proteins.

The Flp-In T-Rex 293 cell line contains a single stably integrated FRT site in a transcriptomic active genomic locus and a randomly integrated tetracycline transactivation gene (tTA). The pcDNA5-FRT/TO-FLAG-BirA$^{*(R118G)}$ expression vector used to generate the fusion proteins contains a hygromycin cassette that does not have starting codon and it is out of frame (**Figure 4**). After the FLP recombination event the opening reading frame (ORF) of the hygromycin cassette in the expression vector gets in frame with the promoter conferring hygromycin resistance to the cells. In addition to the hygromycin cassette, this expression vector contains a tetracycline-controlled promoter, commonly classified as Tet-Off system. The plasmid carries TetO operator sequences upstream the CMV promoter where the tTA can bind and repress vector expression (**Figure 4**). The vector expression is induced when tetracycline is supplemented to the media or when the plasmid is expressed in cells that lack tTA.

The protein constructs generated with this plasmid, in addition to the BirA enzyme, they also contain a Flag tag at the N-terminus that can be utilized to visualize the protein construct by immunofluorescence and western blot (**Figure 4**).

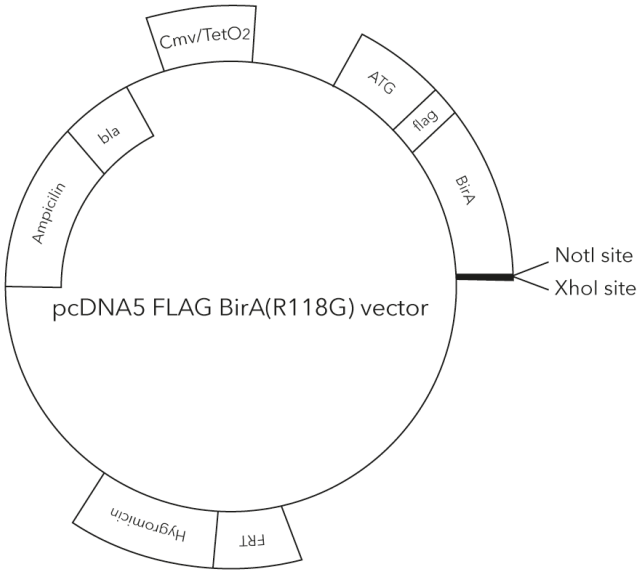

Figure 4 pcDNA5-FRT/TO-FLAG-BirA$^{*(R118G)}$ plasmid map. *Diagram of the expression vector used in this project to create the protein constructs BirA-NUAK2, BirA-CCRK and BirA-GFP respectively. The promoter of the*

vector is CMV with TetO operator sequences upstream where the tetracycline transactivator (tTA) can bind. The fusion protein contains a Flag tag in the N-terminus that can be utilized for functional validation. The vector also contains an ampicillin resistance cassette for bacterial selection and a hygromycin resistance cassette for generation of stable cell lines using Flp recombination.

3.2 Plasmids

Along with BirA-NUAK2 DNA construct, I also generated BirA-CCRK (as it was of interest for an independent project in the lab) and BirA-GFP to use as control for ubiquitous proteins.

Plasmid Name	Information	Purpose
pDEST27 - Hs - NUAK2	Mammalian expression vector. It carries a human NUAK2 CDS.	Template used to subclone NUAK2 CDS.
pDEST27 - mm - CCRK	Mammalian expression vector. It carries a mouse CCRK CDS.	Template used to subclone CCRK CDS.
pcDNA6.2 - emGFP	Mammalian expression vector. It carries a GFP CDS.	Template used to subclone GFP CDS.
pcDNA5-FRT/TO-FLAG-BirA$^{*(R118G)}$	Mammalian expression vector. Confers hygromycin resistance once the FRT site is recombined. CMV promoter, tetracycline inducible.	Destination vector used to generate BirA fusion proteins.
pOG44	Mammalian expression vector. It carries the Flp recombinase CDS.	Generation of stable cell lines.

Table 1: Plasmids used in this project*. CDS stands for coding DNA sequence.*

3.3 PCR primers

ID	Oligo Sequence (written from 5´to 3´ direction)
NotI_Hs_NUAK2_F	GAATTC**GCGGCCGC**GATGGAGTCGCTGGTTTTCG
XhoI_Hs_NUAK2_R	ACGGAG**CTCGAG**TCAGGTGAGCTTTGAGCA
NotI_GFP_F	ACGAAT**GCGGCCGC**CATGGTGAGCAAGGGCGAGGA
SalI_GFP_R	ATTCGT**GTCGAC**TTACGTTTCTCGTTCAGCTT
NotI_Mm_CCRK_F	ACGAAT**GCGGCCGC**CATGGACCAGTATTGCATCCT
SalI_Mm_CCRK_R	ATTCGT**GTCGAC**TCACCCCTCTGGGATGAAGGG

Table 2: Primers used in this project. *First column indicates name of the primer with the restriction site sequence added and origin of the gene CDS; human (Hs) or mouse (Mm). All sequences are written in 5´to 3´direction. Restriction enzyme site highlighted in bold.*

3.4 Restriction enzymes

Restriction enzyme name	Sequence site	Purpose
HindIII	A/AGCTT	Restriction enzyme analysis
NcoI	C/CATGG	Restriction enzyme analysis
NotI	GC/GGCCGC	Cloning
SalI	G/TCGAC	Cloning
XhoI	C/TCGAG	Cloning

Table 3: Restriction enzymes used in this project. *All restriction enzymes are from New England Biolabs (NEB).*

3.5 Cell culture media

If not mentioned otherwise, all mammalian cell lines used in this project were cultured in Dulbecco's Modified Eagle Medium (DMEM) supplemented with 10% fetal bovine serum (FBS), 1% L-Glutamine and 1% penicillin/streptavidin mix (*hereon* called complete media). Cell cultures were incubated at 37°C 5% CO_2.

3.6 Plasmid extraction

Starter bacterial cultures (*E.Coli DH5α*) carrying the plasmids of interest (**Table 1**) were incubated overnight in lysogeny broth (LB) liquid medium supplemented with 100 μg/ml ampicillin using a shaker incubator (37°C 5% CO_2). Bacterial cells were harvested by centrifugation (8000 rpm, 3 min, at room temperature (RT)). Cell lysis and plasmid extraction was done using a commercial spin column kit (QIAprep Spin Mniprep Kit #27104) following manufacturer's instructions. DNA was eluted in TE buffer (10mM Tris pH 8.0, 1mM EDTA) to a final volume of 50 μl and stored at 4°C. Sample quality and quantity was assessed using Nanodrop.

3.7 PCR cloning

Primer3 software (Untergasser et al., 2012) was used to design forward and reverse primers to amplify and obtain the coding DNA sequences (CDS) of NUAK2, CCRK and GFP, from expression plasmids provided by the lab (**Table 1**). A restriction enzyme site for NotI and XhoI at the 5' and 3' ends of the

forward and reverse primer was added respectively. Due to an inner XhoI site in the CDS of CCRK and GFP a compatible enzyme, SalI was used instead. SalI recognizes a slightly different DNA sequence (**Table 3**) but after cutting the DNA, it creates the same sticky ends than XhoI, therefore it can be used along with XhoI digested DNA products. PCR reactions were done in a final volume of 50 µl using the DNA polymerase Phusion (2mM NTPs, 10uM forward and reverse primers, 1X Phusion HF Buffer, 1.0 units of Phusion enzyme NEB #M0530 and 200-250 ng of template), a termoresistant enzyme with proofreading capacity, to reduce probability of adding mistakes in the sequence that could affect downstream restriction enzyme reactions and subsequent cloning. The thermocycler programs used for each PCR reaction can be found in **Appendix A.** The PCR products were purified from PCR incomplete products by running the samples in 1% agarose gels. The right PCR product band was cut from the gel and purified using the commercial QIAquick Gel extraction kit. Sample quality and concentration was measured using Nanodrop.

3.8 Enzyme digestion and ligation

1 µg of the destination vector, pcDNA5-FRT/TO-FLAG-BirA$^{*(R118G)}$, was digested in a sequential manner due to close proximity of NotI and XhoI restriction enzyme sites (10 base pairs). The vector was incubated 1 h at 37°C with NotI in a total reaction of 30 µl (1X NEB buffer 3.1, 1.0 unit NotI NEB #R0189) followed by 1 h at 37°C with XhoI in a total volume of 50 µl (1X NEB buffer 3.1, 1.0 units XhoI NEB #R0146). Salts were adjusted to the second reaction volume respectively. After digestion, the vector was dephosphorylated to reduce the amount of false positive clones due to re-ligation events using shrimp alkaline phosphatase (SAP).

PCR products were double digested, 1 h at 37°C with NotI and XhoI added simultaneously in a 50 µl reaction. All enzymes were heat inactivated at the end by incubating the reactions 20 min at 65°C.

Ligation reactions were done using the T4 DNA ligase (NEB #M0202) in 10 µl reactions with a molar ratio of 1:3 vector to insert, and set overnight at 16°C in a thermocycler.

3.9 Transformation

E.Coli DH5a competent cells were transformed with the different ligation products by heat-shock inactivation procedure. In brief, competent cells were thawed on ice for 10 min and 2 µl of ligation product (~100 ng) was added to the cells mixing without vortexing nor pipetting the cells, only by swirling the tip of the pipette. Cells were left standing on ice for 30 min and then heat shocked at 42°C for 45 seconds using a heat block and placed back on ice for 5 min. 250 µl of Super Optimal Broth medium (SOC) was added to cells and cultures were incubated for 1 h in a shaker (250 rpm, 37°C). Finally, 100µl

of cell mixture was plated on LB agar plates supplemented with 100 μg/ml ampicillin and left overnight in an incubator at 37°C. Screening for positive colonies carrying the plasmid of interest was assessed by restriction enzyme analysis (**Table 3**).

3.10 Transient transfections

20000 HEK293 cells were plated in 6 cm^2 well plates in complete media without antibiotics and transfected the next morning with the pcDNA5-FRT/TO-FLAG-BirA$^{*(R118G)}$ – NUAK2/CCRK/GFP vector respectively using Lipofectamine2000 following manufacturer's instructions (ThermoFisher). Media was changed to complete media 4 h after transfection. Next day, cells were supplemented with 50 μM biotin and incubated 24 h before protein extraction.

3.11 Immunofluorescence staining

For immunofluorescence staining, 200000 HEK293 cells were plated on collagen coated coverslips overnight and transient transfected with the plasmids of interest next day. 4 h after transfection, media was complemented with 50 μM biotin and kept 24 h. Cells on coverslips were washed twice with PBS to remove free biotin and fixed by incubating 10 min with 4% PFA. To make cell membranes permeable to antibodies, the samples were treated with 0.1 % triton (diluted in PBS) for 10 min and to reduce background signal, samples were blocked 1 h at RT with 5% goat serum (diluted in PBS). Afterwards, samples were incubated 1 h at RT with anti-Flag (1:500 Sigma #F9291) followed by three PBS washes of 5 min each, and 1 h incubation at RT with the secondary antibody (1:400 Alexa fluor 594 anti-mouse). Samples were washed 5 min in PBS, stained 2 min with Hoechst (0.5 μg/ml) and washed again with PBS. Coverslips were mount with mowiol and stored at 4 ºC until imaged. Imaging was done using a Zeiss Axioplan 2 upright epifluorescence microscope. ImageJ was used to extract .tiff and merged color images from .zvi files.

3.12 Protein extraction and immunoblotting

HEK 293 cells were lysed using boiling SDS buffer (Tris 125mM pH 6.8, 2.5% SDS), kept at 90 ºC during 10 min to denaturize all proteins and inactivate proteases and further homogenized by passing the samples through a 27 G needle 8 times. DS-assay was performed to assess protein sample concentrations prior immunoblotting following manufacturer's instructions (BioRad). 20 mg of lysate was loaded in a 10% SDS-PAGE gel, ran 2 h at 35 mA and transferred to a nitrocellulose membrane using wet blotting (1.5 h, 200 mA at 4 ºC). Membranes were blocked with 5% non-fat milk in TBST buffer (TBS, 0.1% tween 20) for 1 h at RT and left overnight incubating in a rotator with the primary antibody at 4°C (1:2000 anti-Flag M2 mouse, Sigma #F9291). Membranes were incubated with HRP-based secondary

antibodies 1 h at RT (HRP-anti-sreptavidin or HRP-anti-mouse accordingly at 1:5000 dilutions in 5% non-fat milk in TBST buffer). Triple TBST washes of 15 min were done between antibody incubations and prior film exposure. Supersignal femto chemiluminiscence reagents (ThermoFisher Scientific #34095) diluted 1 to 10 ml in TBS were used to expose membranes to films.

3.13 Generation of stable cell lines

Fuge6 transfection reagent (Promega #E2691) was used for double transfection of the Flp-In T-Rex 293 cells with the pOG44 vector (vector carrying the Flipase recombinase) and the generated pcDNAFLAG-BirA carrying the fusion constructs of interest, following manufacturer's instructions. Hygromycing selection was started 3rd day after transfection. The cells were kept in selection media until the plates were confluent (~1 month) passaged twice and frozen in 90% FBS, 10% DMSO media. Criovials were stored at -135ºC.

3.14 BioID assay

Six confluent 15 cm^2 dishes of FlpIn T-Rex 293 cells for each experimental condition were used as starting material for the BioID assay. When plates were 80% confluent, cells were incubated 24 h with 50 μM biotin and 1μg/mL tetracycline in complete media to express the BirA-construct and induce BirA activity (as recommended by Roux et al. 2012). Cells were rinsed twice with PBS to remove free biotin from the medium before adding SDS cell lysis buffer (50 mM TrisCl pH 7.4, 500 mM NaCl, 0.2% SDS, 1x protease inhibitor cocktail and 1mM DTT added just before use), scraped and harvested in eppendorf tubes, one for each condition (all carried on ice). The cell lysate was transferred to a 15 mL canonical tube and 240 μl of 20% Triton X-100 was added and mixed by trituration. Samples were sonicated (2 sessions with 30 pulses) and afterwards 2 ml of prechilled 50 mM TrisCl pH 7.4 was added and mixed to increase favorable conditions for affinity capture. Sample was aliquoted evenly into 3 prechilled 2-ml tubes and spin down 10 min at 13000 rpm at 4°C. Meanwhile, 2-ml tubes were placed to a magnetic separation stand and filled with 0.75 ml of RT lysis buffer and 0.75 ml of RT 50mM TrisCl, pH 7.4. Streptavidin magnetic beads (Dynabeads MyOne Streptavidin C1, Invitrogen #65001) were resuspended by pipetting. 200 μl of streptavidin beads was added to each tube and let stand in the magnetic separation stand 3 min at RT. Once all the beads were accumulated on one side of the tube wall, the supernatant was removed by pipetting. After sample centrifugation, the supernatant was carefully transferred to the tubes on the magnetic stand, re-suspended along with the beads and let overnight incubating on a rotator at 4°C. Next day streptavidin beads were washed incubating the beads a total of 3 times, 8 min each, in a rotator with a serial of wash buffers, each one containing a smaller fraction of detergents to a final 1.5 ml 50mM TrisCl, pH7.4 (first wash buffer contained 2% SDS. Second wash buffer had 0.1% deoxycholic

acid, 1% Triton X-100, 1mM EDTA, 500 mM NaCl, 50 mM HEPES, pH 7.5 and the final wash buffer had 0.5% deoxycholic acid, 0.5% NP-40, 1mM EDTA, 250mM LiCl and 10 mM TrisCl, pH 7.4). A magnetic stand was used between each wash to successfully remove the supernatant without losing the streptavidin beads.

3.15 Data analysis

Purified biotinylated proteins were sent to be analyzed by liquid-chromatography mass-spectrometry (LC-MS/MS) and protein identification at the Proteomics Unit of the University of Helsinki. The Proteomics Unit prepared the samples for mass-spectrometry, including separation from the streptavidin beads and trypsinization. SEQUEST search algorithm in Proteome Discoverer software (ThermoFisher Scientific) was used for peak extraction and MaxQuant software for protein identification (Cox and Mann, 2008).

For this study, three other datasets created in the lab were also included as controls (**Figure 7A**) to subtract background proteins from NUAK2 dataset with the assumption that the proteins studied had independent function and localization with NUAK2. All the data processing was done uploading the excels provided by the Proteomics Unit to R/Bioconductor platform. A protein identified in NUAK2 dataset was considered specific for NUAK2 if it was not found in any of the other datasets or if the ratio of spectral counts was 3 fold higher than in any other dataset (as suggested by Roux et al. 2012).

4 Results

4.1 Functional validation of fusion constructs and stable cell lines generated.

293 HEK cells were transiently transfected with vectors carrying the different DNA constructs generated (BirA-NUAK2, BirA-CCRK and BirA-GFP respectively) and containing a Flag tag at the N-terminus of the BirA part. Subsequent immunofluorescence staining with anti-Flag demonstrated cytoplasmic staining in a subset of the transiently transfected cells as expected. Based on the analysis the BirA-NUAK2 plasmid showed lower transfection efficiency compared to the other constructs, which may be due to bigger size of the plasmid. As expected, the GFP signal in the BirA-GFP transfection overlapped with the anti-Flag signal (**Figure 5**).

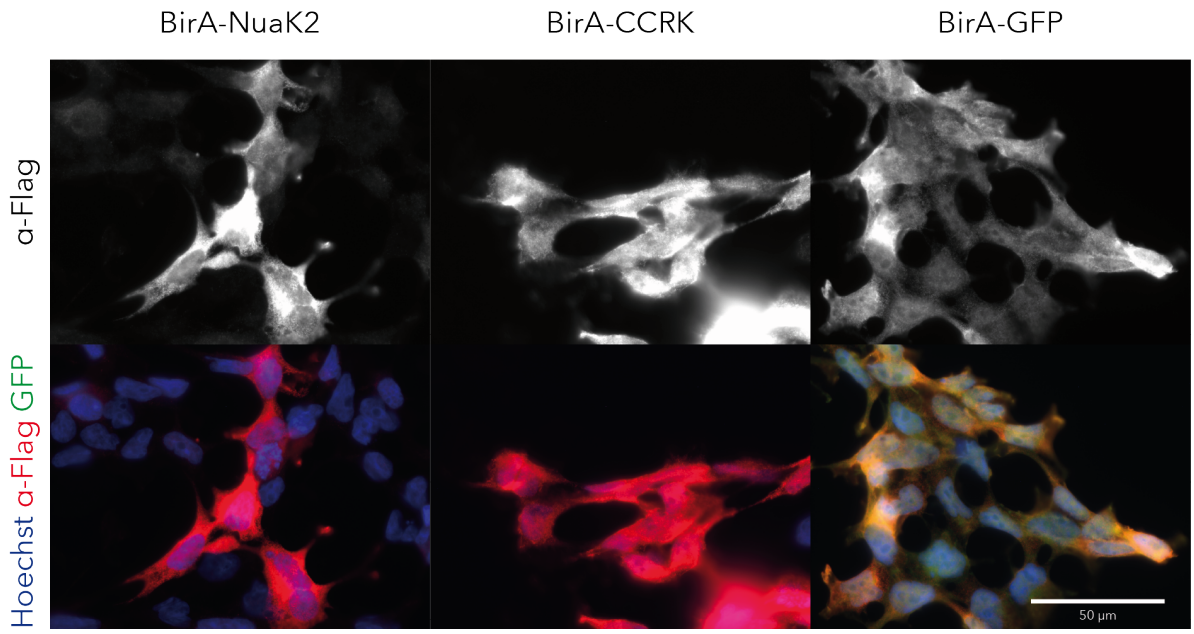

Figure 5: Immunofluoresence analysis of 293 HEK cells transiently transfected with the indicated BirA fusion constructs. *Anti-Flag staining and overall images with nuclear staining (Hoechst) and GFP in case of the BirA-GFP fusion construct.*

Induction of the generated stable HEK293 lines expressing BirA-NUAK2 when supplemented with tetracycline was validated by western blot, using cell lysates of cells previously cultured 24 h with media supplemented with or without 50 µM biotin and 1 µg/ml tetracycline (**Figure 6**). As expected, BirA was only capable of biotinylating proteins when the media was supplemented with both, tetracycline and biotin (**Figure 6**). It should be noted that due to the fusion construct, the fusion protein itself gets

highly self-biotinylated and this can be already spotted in the streptavidin-HRP western blots (red arrows **Figure 6**). From the three stable cell lines generated, BirA-NUAK2 had the lowest overexpression compared to the other constructs (α-Flag **Figure 6B**), being BirA-GFP the highest expressed. In fact, BirA-GFP also showed some residual expression in conditions where the gene should not be expressed (green arrows **Figure 6**). This is likely due to differences in expression and binding of the tetracycline repressor as the repressor gene is randomly integrated in the genome of the Flp-In T-Rex 293 cells when these are generated, and they can be under different promoters. The bands observed in all the conditions where the plasmid is not expressed nor biotin is supplemented are endogenous biotinylated proteins.

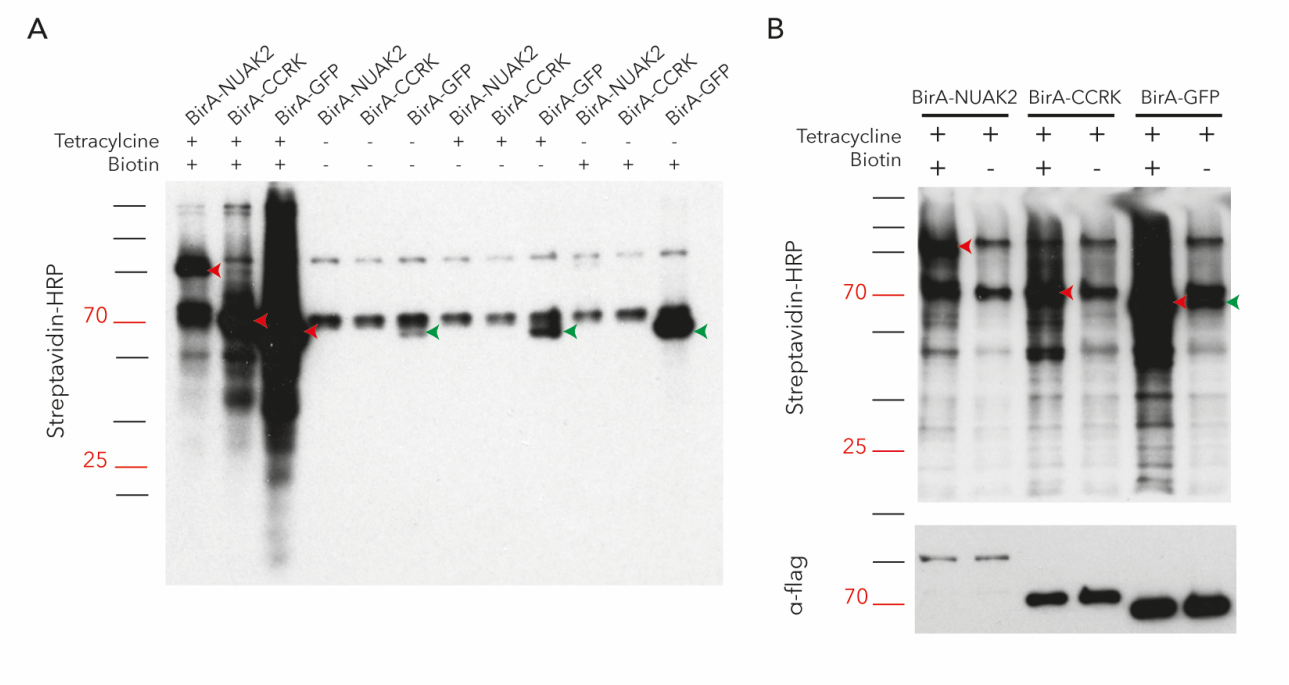

Figure 6: Immunobloting of the stable 293 FlpIn TRex cell lines generated. A, B. *Streptavidin-HRP and anti-Flag blotting of protein cell lysates from BirA-NUAK2, BirA-CCRK and BirA-GFP 293 HEK FlpIn T-Rex cell lines supplemented 24h with or without 50 μM biotin, 1μg/ml tetracycline. Red arrow indicates band likely to be the self-biotinylated construct (BirA-NUAK2 109kDa, BirA-CCRK 78 kDa, BirA-GFP 68 kDa respectively). Green arrows indicate BirA-GFP protein expression leakage.*

4.2 BioID assay with BirA-NUAK2 identified previously known protein-protein NUAK2 interactions as well as potential new candidates.

Biotinylated proteins from cells lysates were purified using streptavidin magnetic beads and mass-spectrometry analysis was carried out in the Proteomics Unit from the University of Helsinki. The output was joined with other datasets produced independently in the lab (**Figure 7A**). Each dataset was used as

control of the other datasets to remove background proteins with the assumption that each protein has independent functions, and therefore they would not share any substrate. Any shared protein identified between datasets was considered background, ubiquitous protein, unless one of the datasets had a 3 fold higher spectral count than the other, following original paper recommendations.(Roux et al., 2012). Taking BirA-NUAK2 dataset as reference, the different proteins identified after background removal were narrowed down from 694 to 108 (**Figure 7B**).

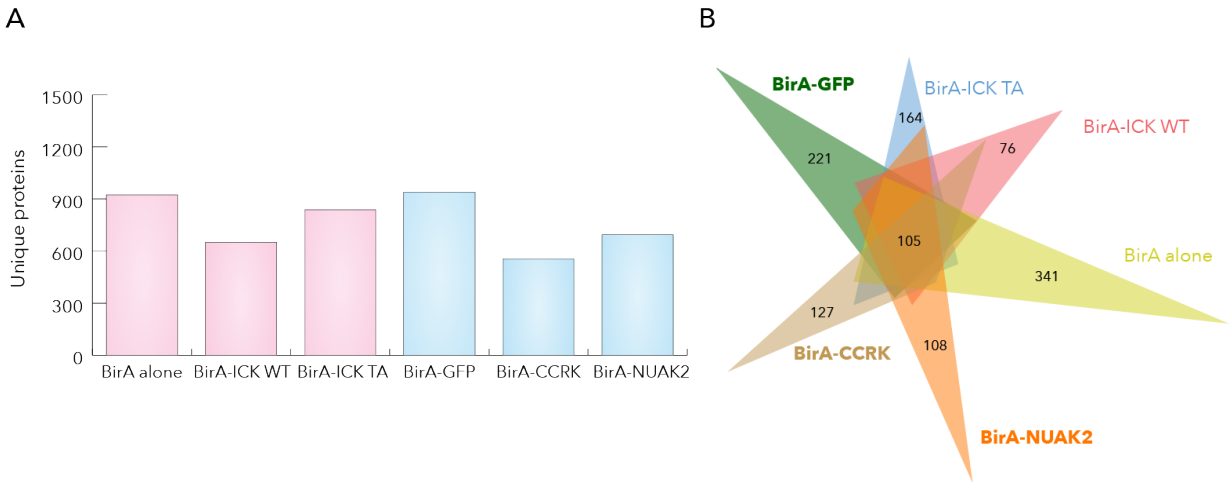

Figure 7: BioID datasets used in this project. A. *Number of different proteins identified in each BirA fusion construct dataset. Indicated in blue the datasets generated in this thesis. In pink, datasets included as controls but not generated in this study.* ***B****. Venn diagram with the overlaps between datasets (created with Jvenn web-tool, Bardou et al. 2014). The diagram only shows the total shared overlap number and the result of subtracting all shared overlaps per each dataset.*

Ranking this list by abundance of unique peptide hits identified for each protein group it was promising to see in the top 3 of the list the two previously published interactions with NUAK2, MYPT1 and MRIP, in first and second place respectively, followed by NUAK2 itself (**Table 4**) (Vallenius et al., 2011; Yamamoto et al., 2008). Self-biotinylation events of the fusion construct were expected as it is the closest protein to BirA and in the western blots it was already visible (red arrows in **Figure 6**). In lower ranks but in high abundance 14-3-3 proteins and several phosphatase catalytic subunits from the MLC phosphatase complex were also detected. As already mentioned, recruitment of 14-3-3 by phosphorylation of MYPT1 is one of the mechanisms to inhibit the phosphatase's recruitment to actin stress fibers and subsequent dephosphorylation of MLC (Koga and Ikebe, 2008).

Importantly for the aim to identify new interactors the screen identified 108 new potential interactors. Interestingly, these include highly ranked proteins previously linked with functions of interest

regarding NUAK2 such as Cytospin-A, Serpin B4 and Serpin B3 (**Table 4**), ranking higher than 14-3-3 and PP1 regulatory subunits. Cytospin-A is a crosslinking protein between actin stress fibers and microtubules.

Rank	Accession	Protein name	Description
1	**O14974**	**MYPT1**	**Protein phosphatase 1 regulatory subunit 12A**
2	**Q6WCQ1**	**MRIP**	**Myosin phosphatase Rho-interacting protein**
3	Q9H093	NUAK2	NUAK family, SNF1-like kinase 2
4	Q69YQ0	CYTSA	Cytospin-A
5	P62140	PP1B	Serine/threonine-protein phosphatase PP1-beta catalytic subunit
6	P48594	SPB4	Serpin B4
7	P29508	SPB3	Serpin B3
8	P31947	1433S	14-3-3 protein sigma
9	Q9BZL4	PP12C	Protein phosphatase 1 regulatory subunit 12C
10	Q8IXQ4	GPAM1	GPALPP motifs-containing protein 1
11	P20671	H2A1D	Histone H2A type 1-D
12	Q96HR8	NAF1	H/ACA ribonucleoprotein complex non-core subunit NAF1
13	O60237	MYPT2	Protein phosphatase 1 regulatory subunit 12B
14	P01857	IGHG1	Ig gamma-1 chain C region
15	O15446	RPA34	DNA-directed RNA polymerase I subunit RPA34

Table 4: Top 15 proteins identified by BioID of BirA-NUAK2 fusion construct. *Ranked by number of unique peptides identified for each protein group. Shaded in blue, proteins of the MLC phosphatase complex and associated proteins. In bold previously known partners of NUAK2. Shaded in yellow, potential new interactors of NUAK2.*

5 Discussion and conclusions

Little is known about the biological relevance of the NUAK2 kinase and its involvement in LKB1 tumorigenesis, in part due to limited knowledge of its protein-protein interactions. In this project, I generated a stable cell line expressing an inducible vector carrying a BirA-NUAK2 fusion protein and utilized the BioID method to successfully identify new protein-protein associations as well as previously known interactions.

All the subunits of the MLC phosphatase and classic associated proteins like 14-3-3 were found in the top 15 of the ranked proteins identified with the BioID method (**Table 4**). This clearly indicated NUAK2 is localized around the MLC phosphatase complex. It should be mentioned that the results were from a single experiment, without replicates, and this could increase false positives. However, the fact that previously known interactions, MYPT1 and MRIP, were the two most biotinylated proteins by BirA-NUAK2, ranking higher than self-biotinylation events, gives us confidence to trust the results. The screening also identified three new potential protein-protein associations discussed more in detail below (**Table 4**). A technical comment, BirA-GFP and BirA alone constructs were used to try to identify ubiquitous proteins. However, both of these constructs had very high levels of overexpression. BirA-GFP was detected in conditions where the gene expression or BirA activity was not induced (as marked with green arrows in **Figure 6**). Moreover, likely due to small size and to the fact that these constructs do not localize to any particular location inside the cell, a big fraction of proteins identified by the BioID were not shared with the other BirA protein constructs (**Figure 7B**). Interestingly, background removal of ubiquitous proteins using as control independent kinases (like BirA-CCRK and BirA-ICK) proved to be very successful as it detected the same fraction of ubiquitous proteins than BirA-GFP or BirA alone (~100) with the additional advantage of revealing biological information regarding their own protein-protein associations. With these results, I would recommend to use independent proteins as internal controls for each other, rather than a ubiquitous construct like BirA-GFP, for further studies.

The most promising candidate, ranked in 4th position, was Cytospin-A (**Table 4**). Cytospin-A is a crosslinking protein that has not been extensively studied. Cytospin-A was one of the genes identified mutated in oblique facial clefts (Saadi et al., 2011). This congenital facial malformation is caused partly due to failure in epithelial-mesenchymal transdifferentiation, and therefore abnormal cell-cell detachment during delamination of the cranial neural crest cells (Saadi et al., 2011; Wilson et al., 2016). Cells lacking Cytospin-A had increased adherent junctions stability indicated by increased E-cadherin and β-catenin at the junctions (Wilson et al., 2016). These cells also showed increased actin stress fibers but they were randomly organized and more prominent in the middle of the cell. Cytospin-A was characterized as a

crosslink associated protein between microtubules and actin cytoskeleton because overexpression in cells co-localized with both, tubulin and actin, stabilizing microtubules (Saadi et al., 2011). It is suggested that Cytospin-A may mediate transduction of signals required to reorganize actin stress fibers during cell adhesion (Saadi et al., 2011). It is too early to speculate the role of this protein in NUAK2-dependent actin stress fibers reorganization but it could be assessed using the NUAK2 actin stress remodeling phenotype as a functional assay. The CDS of Cytospin-A is commercially available and it could be subcloned and used in overexpression assays and also co-immunoprecipitation to validate the interaction with NUAK2.

Other promising candidates include proteases inhibitors, SERPINB3 and SERPINB4 respectively. They both have been found overexpressed in many advanced carcinomas and idiopathic pulmonary fibrosis (Calabrese et al., 2012; Turato et al., 2014). In particular, SERPINB3 has been shown to protect tumor cells from apoptosis by inhibiting release of cytochrome c from the mitochondria (Vidalino et al., 2009). It is not evident in this case how to investigate its putative association with NUAK2 as currently there is no functional assay to work on. The CDS of these protease inhibitors are also available so validation of the physical interaction could be approached by co-immunoprecipitation or cross-linking protein interaction assays. Optimization of these methods is usually demanding but the approach would validate the interaction with NUAK2.

Interestingly, NUAK1 was not found in the whole dataset. It has been shown to be associated to MLC phosphatase and inactivate the MYPT1 by phosphorylation (Zagórska et al., 2010) and therefore, should localize quite close to NUAK2. However, it was not detected in the whole screen (nor before subtracting background proteins). This negative result could be due to low protein levels of endogenous NUAK1 or allosteric interactions that could have kept NUAK1 out of reach from BirA biotinylation. There is no evidence that NUAKs associate in a complex to perform their functions and this negative result would not point to that direction. In any case, further validation of the protein interactions with NUAK2 should also include NUAK1 as these two kinases are closely related and they could still share many of their biological functions and protein partners.

As far as the protein-protein associations discussed the dataset is quite narrow and the spectral counts and coverage of the proteins identified drops quickly below the top 15. Since previous literature shows NUAK2 regulation and functions appear to be cell type and context dependent, it could reveal more information to use the BioID method with cells under different cellular stress conditions as well as in different cell types. This could reveal if NUAK2 versatility is due to different protein-protein associations or if the different functions described for NUAK2 are linked at a molecular level.

In conclusion, in this project I created a BirA-NUAK2 protein construct and generated an inducible 293 cell line that expressed the fusion protein after media supplementation with tetracycline. I tested by immunoblotting and immunofluorescence that the BirA-NUAK2 was functional and that BirA was able to biotinylate vicinity proteins after addition of biotin to the media. Finally, I utilized a proximity-dependent biotin labeling method, the BioID, to identify novel protein-protein associations. The screening identified previously known protein interactions, MYPT1 and MRIP, and also 108 new candidates, including Cytospin-A interesting due to its association and effect on actin stress fibers. The results thus provide potential new information on NUAK2 biology and may provide tools to study its role in tumorigenesis. Validation of the protein-protein interactions and their potential role in NUAK2 functions should be addressed in the future e.g. by using NUAK2-dependent actin stress fibers remodeling phenotype as a functional assay and by co-immunoprecipitation methods.

6 Acknowledgments

This Master's thesis was carried out in the University of Helsinki under the Master's Degree Program of Biotechnology (MBIOT) from the faculty of Biological and Environmental Sciences.

First, I would like to express my deepest gratitude to my supervisor Tomi Mäkelä for accepting me in his lab and giving me the opportunity to start my journey in the scientific world under his guidance. It is a privilege to learn from you.

I would like to thank all the Mäkelä-lab members, for the great discussions and atmosphere in the lab. I would have not been able to do this project without your advice and support. Special thanks to Saara, your teachings in the daily lab routines as well as your insight in science have been very helpful. Working together is a blessing. I am looking forward to the projects that lie ahead.

I am indebted to my parents for their endless support and trust in me. Your advice and values you have taught me are a big part of who I am. I want to thank also my sister Sara, your endless creativity to make me see the silver lining every time challenges blinded me is priceless. Last but not least, I want to thank Essi. There are no words to express how lucky I feel that you made me part of your life.

Thanks to all,

Helsinki, 28th of May 2017

7 References

Bardou, P., Mariette, J., Escudié, F., Djemiel, C., and Klopp, C. (2014). jvenn: an interactive Venn diagram viewer. *BMC Bioinformatics*, *15*, 293.

Calabrese, F., Lunardi, F., Balestro, E., Marulli, G., Perissinotto, E., Loy, M., … Rea, F. (2012). Serpin B4 isoform overexpression is associated with aberrant epithelial proliferation and lung cancer in idiopathic pulmonary fibrosis. *Pathology*, *44*(3), 192–198.

Cox, J., and Mann, M. (2008). MaxQuant enables high peptide identification rates, individualized p.p.b.-range mass accuracies and proteome-wide protein quantification. *Nature Biotechnology*, *26*(12), 1367–1372.

Firat-Karalar, E. N., Rauniyar, N., Yates, J. R., and Stearns, T. (2014). Proximity interactions among centrosome components identify regulators of centriole duplication. *Current Biology*, *24*(6), 664–670.

Fleuren, E. D. G., Zhang, L., Wu, J., and Daly, R. J. (2016). The kinome "at large" in cancer. *Nature Reviews Cancer*, *16*(2), 83–98.

Fu, Y., Lv, P., Yan, G., Fan, H., Cheng, L., Zhang, F., … Wen, B. (2015). MacroH2A1 associates with nuclear lamina and maintains chromatin architecture in mouse liver cells. *Scientific Reports*, *5*, 17186.

Fujii, N., Hirshman, M. F., Kane, E. M., Ho, R. C., Peter, L. E., Seifert, M. M., and Goodyear, L. J. (2005). AMP-activated Protein Kinase 2 Activity Is Not Essential for Contraction- and Hyperosmolarity-induced Glucose Transport in Skeletal Muscle. *Journal of Biological Chemistry*, *280*(47), 39033–39041.

Giardiello, F. M., Brensinger, J. D., Tersmette, A. C., Goodman, S. N., Petersen, G. M., Booker, S. V., … Offerhaus, J. A. (2000). Very high risk of cancer in familial Peutz–Jeghers syndrome. *Gastroenterology*, *119*(6), 1447–1453.

Goodyear, L. J., and Kahn, B. B. (1998). Exercise, glucose transport, and insulin sensitivity. *Annual Review of Medicine*, *49*(1), 235–261.

Grangeasse, C., Nessler, S., and Mijakovic, I. (2012). Bacterial tyrosine kinases: evolution, biological function and structural insights. *Philosophical Transactions of the Royal Society B: Biological Sciences*, *367*(1602), 2640–2655.

Hardie, D. G. (2007). AMP-activated/SNF1 protein kinases: conserved guardians of cellular energy.

Nature Reviews Molecular Cell Biology, *8*(10), 774–785.

Hoppe, P. E., Chau, J., Flanagan, K. A., Reedy, A. R., and Schriefer, L. A. (2010). *Caenorhabditis elegans unc-82* Encodes a Serine/Threonine Kinase Important for Myosin Filament Organization in Muscle During Growth. *Genetics*, *184*(1), 79–90.

Jeppesen, J., Maarbjerg, S. J., Jordy, A. B., Fritzen, A. M., Pehmøller, C., Sylow, L., … Kiens, B. (2013). LKB1 Regulates Lipid Oxidation During Exercise Independently of AMPK. *Diabetes*, *62*(5), 1490–1499.

Ji, H., Ramsey, M. R., Hayes, D. N., Fan, C., McNamara, K., Kozlowski, P., … Wong, K.-K. (2007). LKB1 modulates lung cancer differentiation and metastasis. *Nature*, *448*(7155), 807–810.

Jørgensen, S. B., Viollet, B., Andreelli, F., Frøsig, C., Birk, J. B., Schjerling, P., … Wojtaszewski, J. F. P. (2004). Knockout of the α2 but Not α1, 5'-AMP-activated Protein Kinase Isoform Abolishes 5-Aminoimidazole-4-carboxamide-1-β-4-ribofuranoside- but Not Contraction-induced Glucose Uptake in Skeletal Muscle. *Journal of Biological Chemistry*, *279*(2), 1070–1079.

Katajisto, P., Vaahtomeri, K., Ekman, N., Ventelä, E., Ristimäki, A., Bardeesy, N., … Mäkelä, T. P. (2008). LKB1 signaling in mesenchymal cells required for suppression of gastrointestinal polyposis. *Nature Genetics*, *40*(4), 455–459.

Katajisto, P., Vallenius, T., Vaahtomeri, K., Ekman, N., Udd, L., Tiainen, M., and Mäkelä, T. P. (2007). The LKB1 tumor suppressor kinase in human disease. *Biochimica et Biophysica Acta (BBA) - Reviews on Cancer*, *1775*(1), 63–75.

Kim, D. I., Jensen, S. C., Noble, K. A., Kc, B., Roux, K. H., Motamedchaboki, K., and Roux, K. J. (2016). An improved smaller biotin ligase for BioID proximity labeling. *Molecular Biology of the Cell*, *27*(8), 1188–1196.

Kim, D. I., Kc, B., Zhu, W., Motamedchaboki, K., Doye, V., and Roux, K. J. (2014). Probing nuclear pore complex architecture with proximity-dependent biotinylation. *Proceedings of the National Academy of Sciences*, *111*(24), E2453–E2461.

Koga, Y., and Ikebe, M. (2008). A novel regulatory mechanism of myosin light chain phosphorylation via binding of 14-3-3 to myosin phosphatase. *Molecular Biology of the Cell*, *19*(3), 1062–1071.

Koh, H.-J., Arnolds, D. E., Fujii, N., Tran, T. T., Rogers, M. J., Jessen, N., … Goodyear, L. J. (2006).

Skeletal Muscle-Selective Knockout of LKB1 Increases Insulin Sensitivity, Improves Glucose Homeostasis, and Decreases TRB3. *Molecular and Cellular Biology*, *26*(22), 8217–8227.

Koh, H.-J., Toyoda, T., Fujii, N., Jung, M. M., Rathod, A., Middelbeek, R. J.-W., … Goodyear, L. J. (2010). Sucrose nonfermenting AMPK-related kinase (SNARK) mediates contraction-stimulated glucose transport in mouse skeletal muscle. *Proceedings of the National Academy of Sciences*, *107*(35), 15541–15546.

Kreisberg, J. I., Ghosh-Choudhury, N., Radnik, R. A., and Schwartz, M. A. (1997). Role of Rho and myosin phosphorylation in actin stress fiber assembly in mesangial cells. *American Journal of Physiology - Renal Physiology*, *273*(2), F283–F288.

Lefebvre, D. L., Bai, Y., Shahmolky, N., Sharma, M., Poon, R., Drucker, D. J., and Rosen, C. F. (2001). Identification and characterization of a novel sucrose-non-fermenting protein kinase/AMP-activated protein kinase-related protein kinase, SNARK. *Biochemical Journal*, *355*(Pt 2), 297–305.

Lefebvre, D. L., and Rosen, C. F. (2005). Regulation of SNARK activity in response to cellular stresses. *Biochimica et Biophysica Acta (BBA) - General Subjects*, *1724*(1–2), 71–85.

Legembre, P., Schickel, R., Barnhart, B. C., and Peter, M. E. (2004). Identification of SNF1/AMP Kinase-related Kinase as an NF-κB-regulated Anti-apoptotic Kinase Involved in CD95-induced Motility and Invasiveness. *Journal of Biological Chemistry*, *279*(45), 46742–46747.

Lessard, S. J., Rivas, D. A., So, K., Koh, H.-J., Queiroz, A. L., Hirshman, M. F., … Goodyear, L. J. (2017). The AMPK-related kinase SNARK regulates muscle mass and myocyte survival. *The Journal of Clinical Investigation*, *126*(2), 560–570.

Lizcano, J. M., Göransson, O., Toth, R., Deak, M., Morrice, N. A., Boudeau, J., … Alessi, D. R. (2004). LKB1 is a master kinase that activates 13 kinases of the AMPK subfamily, including MARK/PAR-1. *The EMBO Journal*, *23*(4), 833–843.

Manning, G., Whyte, D. B., Martinez, R., Hunter, T., and Sudarsanam, S. (2002). The Protein Kinase Complement of the Human Genome. *Science*, *298*(5600), 1912–1934.

Mu, J., Brozinick, J. T., Valladares, O., Bucan, M., and Birnbaum, M. J. (2001). A role for AMP-activated protein kinase in contraction- and hypoxia-regulated glucose transport in skeletal muscle. *Molecular Cell*, *7*(5), 1085–1094.

Namiki, T., Coelho, S. G., Hearing, V. J., Namiki, T., Coelho, S. G., and Hearing, V. J. (2011). NUAK2: an emerging acral melanoma oncogene. *Oncotarget*, *2*(9), 695–704.

Namiki, T., Tanemura, A., Valencia, J. C., Coelho, S. G., Passeron, T., Kawaguchi, M., … Hearing, V. J. (2011). AMP kinase-related kinase NUAK2 affects tumor growth, migration, and clinical outcome of human melanoma. *Proceedings of the National Academy of Sciences*, *108*(16), 6597–6602.

Namiki, T., Yaguchi, T., Nakamura, K., Valencia, J. C., Coelho, S. G., Yin, L., … Hearing, V. J. (2015). NUAK2 Amplification Coupled with PTEN Deficiency Promotes Melanoma Development via CDK Activation. *Cancer Research*, *75*(13), 2708–2715.

Rees, J. S., Li, X.-W., Perrett, S., Lilley, K. S., and Jackson, A. P. (2015). Protein Neighbors and Proximity Proteomics. *Molecular & Cellular Proteomics*, *14*(11), 2848–2856.

Roux, K. J., Kim, D. I., Raida, M., and Burke, B. (2012). A promiscuous biotin ligase fusion protein identifies proximal and interacting proteins in mammalian cells. *Journal of Cell Biology*, *196*(6), 801–810.

Rune, A., Osler, M. E., Fritz, T., and Zierath, J. R. (2009). Regulation of skeletal muscle sucrose, non-fermenting 1/AMP-activated protein kinase-related kinase (SNARK) by metabolic stress and diabetes. *Diabetologia*, *52*(10), 2182–2189.

Saadi, I., Alkuraya, F. S., Gisselbrecht, S. S., Goessling, W., Cavallesco, R., Turbe-Doan, A., … Maas, R. L. (2011). Deficiency of the Cytoskeletal Protein SPECC1L Leads to Oblique Facial Clefting. *The American Journal of Human Genetics*, *89*(1), 44–55.

Stanford, K. I., and Goodyear, L. J. (2014). Exercise and type 2 diabetes: molecular mechanisms regulating glucose uptake in skeletal muscle. *Advances in Physiology Education*, *38*(4), 308–314.

Street, C. A., and Bryan, B. A. (2011). Rho Kinase Proteins—Pleiotropic Modulators of Cell Survival and Apoptosis. *Anticancer Research*, *31*(11), 3645–3657.

Surks, H. K., Riddick, N., and Ohtani, K. (2005). M-RIP Targets Myosin Phosphatase to Stress Fibers to Regulate Myosin Light Chain Phosphorylation in Vascular Smooth Muscle Cells. *Journal of Biological Chemistry*, *280*(52), 42543–42551.

Suzuki, A., Kusakai, G.-I., Kishimoto, A., Lu, J., Ogura, T., Lavin, M. F., and Esumi, H. (2003). Identification of a novel protein kinase mediating Akt survival signaling to the ATM protein. *The*

Journal of Biological Chemistry, *278*(1), 48–53.

Suzuki, A., Kusakai, G., Kishimoto, A., Minegichi, Y., Ogura, T., and Esumi, H. (2003). Induction of cell–cell detachment during glucose starvation through F-actin conversion by SNARK, the fourth member of the AMP-activated protein kinase catalytic subunit family. *Biochemical and Biophysical Research Communications*, *311*(1), 156–161.

Tsuchihara, K., Ogura, T., Fujioka, R., Fujii, S., Kuga, W., Saito, M., … Esumi, H. (2008). Susceptibility of Snark-deficient mice to azoxymethane-induced colorectal tumorigenesis and the formation of aberrant crypt foci. *Cancer Science*, *99*(4), 677–682.

Turato, C., Vitale, A., Fasolato, S., Ruvoletto, M., Terrin, L., Quarta, S., … Pontisso, P. (2014). SERPINB3 is associated with TGF-β1 and cytoplasmic β-catenin expression in hepatocellular carcinomas with poor prognosis. *British Journal of Cancer*, *110*(11), 2708–2715.

Untergasser, A., Cutcutache, I., Koressaar, T., Ye, J., Faircloth, B. C., Remm, M., and Rozen, S. G. (2012). Primer3-new capabilities and interfaces. *Nucleic Acids Research*, *40*(15), e115.

Vaahtomeri, K., Ventelä, E., Laajanen, K., Katajisto, P., Wipff, P.-J., Hinz, B., … Mäkelä, T. P. (2008). Lkb1 is required for TGFβ-mediated myofibroblast differentiation. *Journal of Cell Science*, *121*(21), 3531–3540.

Vallenius, T., Vaahtomeri, K., Kovac, B., Osiceanu, A.-M., Viljanen, M., and Mäkelä, T. P. (2011). An association between NUAK2 and MRIP reveals a novel mechanism for regulation of actin stress fibers. *Journal of Cell Science*, *124*(3), 384–393.

Varnaitė, R., and MacNeill, S. A. (2016). Meet the neighbors: Mapping local protein interactomes by proximity-dependent labeling with BioID. *Proteomics*, *16*(19), 2503–2518.

Vidalino, L., Doria, A., Quarta, S., Zen, M., Gatta, A., and Pontisso, P. (2009). SERPINB3, apoptosis and autoimmunity. *Autoimmunity Reviews*, *9*(2), 108–112.

Wang, B., Yang, S., Zhang, L., and He, Z.-G. (2010). Archaeal Eukaryote-Like Serine/Threonine Protein Kinase Interacts with and Phosphorylates a Forkhead-Associated-Domain-Containing Protein. *Journal of Bacteriology*, *192*(7), 1956–1964.

Wang, Y., Zheng, X. R., Riddick, N., Bryden, M., Baur, W., Zhang, X., and Surks, H. K. (2009). ROCK Isoform Regulation of Myosin Phosphatase and Contractility in Vascular Smooth Muscle Cells.

Circulation Research, *104*(4), 531–540.

Wilson, N. R., Olm-Shipman, A. J., Acevedo, D. S., Palaniyandi, K., Hall, E. G., Kosa, E., … Saadi, I. (2016). SPECC1L deficiency results in increased adherens junction stability and reduced cranial neural crest cell delamination. *Scientific Reports*, *6*, 17735.

Xu, J., Ji, J., and Yan, X.-H. (2012). Cross-Talk between AMPK and mTOR in Regulating Energy Balance. *Critical Reviews in Food Science and Nutrition*, *52*(5), 373–381.

Yamamoto, H., Takashima, S., Shintani, Y., Yamazaki, S., Seguchi, O., Nakano, A., … Kitakaze, M. (2008). Identification of a novel substrate for TNFα-induced kinase NUAK2. *Biochemical and Biophysical Research Communications*, *365*(3), 541–547.

Zagórska, A., Deak, M., Campbell, D. G., Banerjee, S., Hirano, M., Aizawa, S., … Alessi, D. R. (2010). New Roles for the LKB1-NUAK Pathway in Controlling Myosin Phosphatase Complexes and Cell Adhesion. *Science Signaling*, *3*(115), ra25-ra25.

8 Appendices

Appendix A. Thermocycler programs

		Temperature	Time
Initial denaturation		98°C	30 sec
30 cycles	Denaturation	98°C	10 sec
	Annealing	61°C	40 sec
	Extension	72°C	1 min
Final extension		72°C	10 min
Hold		4°C	forever

Thermocycler program for NUAK2 CDS

		Temperature	Time
Initial denaturation		98°C	30 sec
30 cycles	Denaturation	98°C	10 sec
	Annealing	59°C	30 sec
	Extension	72°C	30 sec
Final extension		72°C	10 min
Hold		4°C	forever

Thermocycler program of CCRK and GFP CDS